Deriving time-concordant event cascades from gene expression data: A case study for Drug-Induced Liver Injury (DILI)

Anika Liu[1,2,3*], Namshik Han[1], Jordi Munoz-Muriedas[2], Andreas Bender[3*]

[1] Milner Therapeutics Institute, University of Cambridge, Cambridge, United Kingdom

[2] Systems Modelling and Translational Biology, Data and Computational Sciences, GSK, London, United Kingdom

[3] Centre for Molecular Informatics, Department of Chemistry, University of Cambridge, Cambridge, United Kingdom

[4] Cambridge Centre for AI in Medicine, Department of Applied Mathematics and Theoretical Physics, University of Cambridge, Cambridge, United Kingdom

*Corresponding author
E-mail: ab454@cam.ac.uk (AB), al862@cam.ac.uk (AL)

Abstract

Adverse event pathogenesis is often a complex process which compromises multiple events ranging from the molecular to the phenotypic level. Adverse Outcome Pathways (AOPs) aim to formalize this as temporal sequences of events, in which event relationships should be supported by causal evidence according to the tailored Bradford-Hill criteria. One of the criteria is whether events are consistently observed in a certain temporal order and, in this work, we study this time concordance between gene expression- and histopathology-derived events as data-driven means to generate hypotheses on potentially causal mechanisms. As a case study, we analysed liver data from repeat-dose studies in rats from the TG-GATEs database which comprises measurements across eight timepoints, ranging from 3 hours to 4 weeks post-treatment. We identified time concordant pathway- and transcription factor (TF)- level events preceding adverse histopathology, which serves as surrogate readout for Drug-Induced Liver Injury (DILI). Among known events in DILI, we found some to change strongly before adverse histopathology, e.g. fatty acid beta oxidation, while others were more confident, e.g. bile acid recycling, or frequent, e.g. ATF4-mediated stress response, further characterizing their mechanistic roles. Moreover, we used the temporal order of TF expression and regulon activity to separate induced TFs, such as Cebpa, from post-transcriptionally activated ones, e.g. Srebf2, and subsequently combined this with known functional interactions (TF-target or protein-protein) to derive detailed gene-regulatory mechanisms, such as Hnf4a-dependent Cebpa expression. We additionally evaluate which time concordant events show sustained or increasing activation over time, as this time dependence is favourable for biomarker development, and identify pathways indicating dyslipidaemia, and a decrease in Hnf1a and Hnf4a indicating deteriorating liver function. At the same, time also potentially novel events are identified such as Sox13 which shows a more significant time dependence and -concordance than many known TFs in liver injury. Overall, we demonstrate how time-resolved transcriptomics can derive and support mechanistic hypotheses by quantifying time concordance and how this can be combined with prior causal knowledge, with the

aim of both understanding mechanisms of toxicity, as well as potential applications to the AOP framework. We make our results available in the form of a Shiny app (https://github.com/anikaliu/DILICascades_App), which allows users to query events of interest in more detail.

Author Summary

One key challenge in statistical analysis is to infer causation instead of correlation, in particular in case of observational data. The conserved temporal order of events, their time concordance, is thereby one potential source of evidence and consequentially time-series data is particularly suited to study causal mechanisms. In this study, we present an automatable framework to quantify and characterize time concordance across a large set of time-series, and we apply this concept to gene-expression- and histopathology-derived events derived from the TG-GATEs *in vivo* liver data as a case study. We were able to recover known events involved in the pathogenesis of Drug-Induced Liver Injury (DILI), and identify potentially novel pathway and transcription factors (TFs) which precede adverse histopathology. As complementary sources of evidence for causality, we additionally show how time concordance and prior knowledge on plausible interactions between TFs can be combined to derive causal hypotheses on the TFs' mode of regulation and interaction partners. Overall, the results derived in our case study can serve as valuable hypothesis-free starting points for the development of Adverse Outcome Pathways for DILI, and demonstrate that our approach provides a novel angle to prioritize mechanistically relevant events.

Introduction

Adverse drug reactions are a major reason for compound failure in the clinical trials [1,2] and the significant cause for post-marketing withdrawals. To counter exposing patients to these risks, it is desired to identify adverse events earlier in the individual patient but also in the drug development

process. Mechanistic understanding of how adverse event pathogenesis is crucial in this regard, i.e. to derive early safety biomarkers or *in vitro* assays. However, current understanding of toxicity is largely incomplete, in particular for complex phenotypes such as organ injury which can usually be caused by a wide range of compounds perturbing the biological system at different points mediated through multiple biological scales and entities [3,4].

Multiple interrelated concepts have been introduced to formalize mechanistic knowledge in the context of toxicity including Adverse Outcome Pathways, AOPs [4,5]. These begin with a molecular initiating event (MIE) which describes the first interaction of the compound with the system, e.g. a target protein, which is then linked to the AE through a causal cascade of key events (KEs) on different biological levels, like activation of cellular pathways or changes in the tissue or organ. Thereby, the Organization for Economic Co-operation and Development [6] published three criteria to evaluate causality between events within AOPs based on the original Bradford Hill considerations in the context of epidemiological studies [7] and previous work on the related Mode of Action concept [8]: Biological plausibility, essentiality of key events and empirical support for key event relationships. Empirical support is further separated into time concordance (Event A happens before event B), dose concordance (Event A happens at lower dose than event B) and incidence concordance (The magnitude of event A is larger than that of event B).

Computational approaches can thereby support these predominantly expert- and knowledge-driven mechanistic efforts by prioritizing mechanistically relevant events or by providing additional insight on the relation between an event and a given phenotype. For instance, computationally predicted AOPs (cpAOPs) prioritize plausible events and event relationships as starting points for expert-driven AOP development by integrating functional and statistical associations between biological entities on different levels [9–11]. In contrast, probabilistic quantitative AOPs (qAOPs) provide additional insight on the predictivity of KERs by aiming to predict the adverse event from *in vitro* assays implementing the expert-curated AOP as scaffold [12,13]. Biological readouts, such as transcriptomics, are

particularly suited to study intermediate key events as they provide broad insights into cellular changes which can then lead to the identification of predictive signatures and mechanistically relevant insights, for example in the context of DILI [14–18]. This included studies on the time (and dose) dependence of gene expression-derived events in the context of adverse findings [19,20], so the changes of individual events across changes in time (and dose), and also aimed to predict later adverse findings from fixed early timepoints [14,15]. In contrast, time concordance, which instead aims to identify the order of activation between two events, has not been explored so far as a means to derive mechanistic events and event relationships from gene expression data.

In this study, we hence quantify time concordance across gene expression- derived cellular events and adverse events based on histopathology across wide range of compounds. To do so, we introduce the concept of “first activation” for mechanistic analysis, which focusses only on the earliest timepoint an event can be reliably detected and then orders events within a time-series by their timepoint of first activation (Fig 1A). In contrast to previous time concordance analyses in AOPs which addressed a defined set of KER and known KE [21–23], this analysis derives statistical evidence for temporal concordance across time-series and can do so for any combination of events based on gene expression or histopathology. Although the confidence of these temporal orders per time series is limited by the noisiness of gene expression data and the low time resolution, statistical significance can be evaluated across time series (Fig 1B). Furthermore, it is possible to separate out events which depict general perturbation response but are unspecific, as well as rare events, which are predictive but only observed for a small subset of compounds.

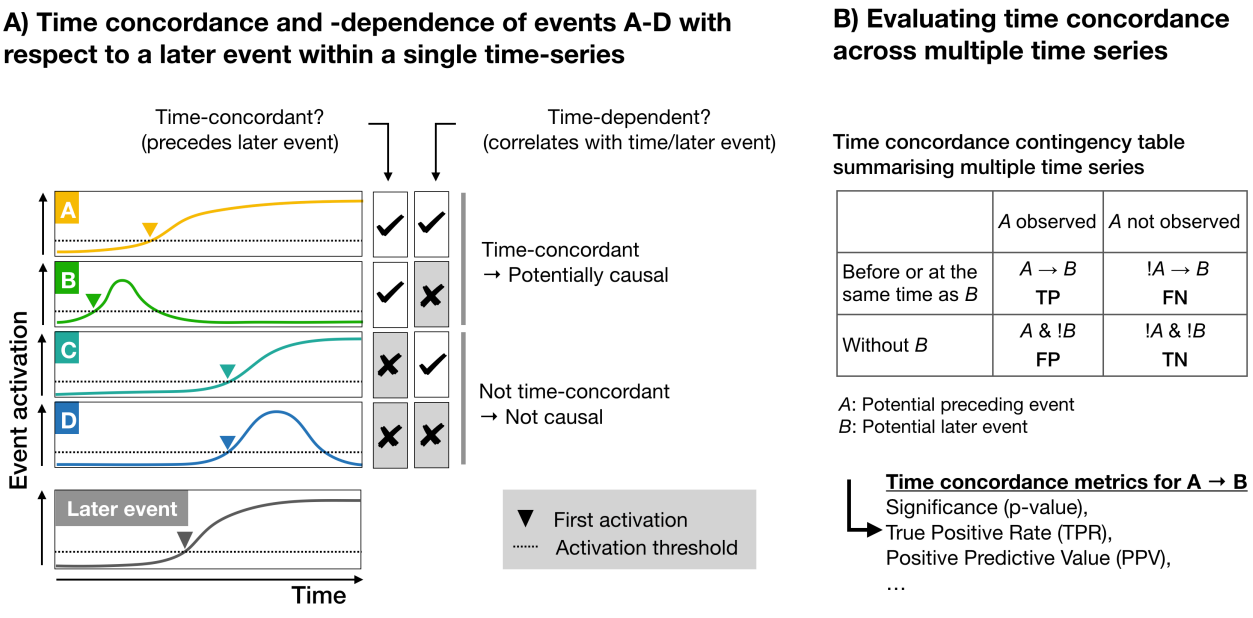

Fig 1 Quantifying time concordance based on first activation. (A) The event activation of the events A-D and the later event is shown over time, as well as their timepoint of first activation, at which the event first passes the defined activation criteria. If an event takes place before a defined later event, which in our study is adverse histopathology, it is time-concordant. Time concordance indicates that there is potentially a causal relation between both events, and is distinct from time-dependence which is defined based on the correlation to the later event or time. (B) Based on the frequency of an event before or at the same time as the later event and its frequency in background time-series without the later event, a confusion matrix and different time concordance metrics can be derived.

We demonstrate the utility of this concept in this work using liver gene expression and histopathology data from repeat-dose studies in rats provided by the TG-GATEs database. This allows us to take advantage of previous data curation and work on the dataset itself, in particular by Sutherland et al. [15] who provide an adverse classification of each compound-dose combination and toxscores summarising histopathological findings in each condition. Furthermore, Drug-Induced Liver Injury (DILI) is well understood in comparison to other organ-level toxicities and we hence know which processes are expected to precede injury, including cell death, inflammation and other adaptive stress responses [24].

We first describe the time concordance for known processes, similar to mechanistic qAOPs, and then prioritize predictive, time-concordant KE providing a strong data-driven, automatable starting point for AOP development, aligning with the objective of cpAOPs (more detailed comparison in S1 Table).

We then combine data-driven time concordance and prior knowledge on event relations between transcription factors (TFs) and gene expression to generate hypothesis for causal gene-regulatory mechanisms in DILI pathogenesis and to generally show how time concordance can stratify and support other streams of causal evidence. Overall, we show that time-resolved gene expression and histopathology data can be used to quantify time concordance across a large set of compounds and events.

Results and Discussion

Adverse histopathological findings and their temporal relation

We firstly evaluated which histopathological findings at which level of magnitude, indicated by toxscore, were frequently found in the adverse compound-dose combinations (observed in at least 5 out of 40 adverse time series) with at least 50% of findings being in adverse time series. Results for all annotated findings are displayed in Fig 2A and the identified adverse histopathological findings include hepatocellular single cell necrosis and biliary hyperplasia at all toxscore thresholds. In contrast, only some of the three toxscore thresholds (“null”, “low”, “high”) were selected with the above criteria for all other findings, e.g. the two higher toxscore cut-offs for hepatocellular necrosis and inflammation and only the “high” cut-off for increased hepatocellular mitosis. In all cases, the lower toxscore level was also frequently observed in non-adverse conditions and hence considered too unspecific. In contrast, only the two milder levels of fibrosis were included in the selection, as severe fibrosis was observed rarely.

For the adverse histopathology labels, the distribution of toxscores and first activation over time (Fig 2B) shows that some findings are predominantly found late, like fibrosis, while others are predominantly found early, e.g. hepatocellular single cell necrosis. This indicates that a further progressed and more severe phenotype tends to be annotated with different terminology. These

adverse histopathology labels were next used to define 61 time-series associated with any of the given histological changes, covering 38 compounds, as adverse (S2 Table). In those, the earliest evidence of an adverse phenotype is used to approximate the timepoint of the primary insult. From this analysis, across all timeseries with adverse histopathology, we find that hepatocellular single cell necrosis is most frequently the primary insult, while biliary hyperplasia at any severity is in most cases a secondary effect (Fig 2C, S2 Fig). Furthermore, higher doses are generally found to induce earlier, and more severe, changes across all findings. We additionally investigated for all histopathology labels how frequently these were observed before or after the primary insult, and for example find vascular edema exclusively before or at the primary insult, and hepatocellular hypertrophy most frequently afterwards (for details see S2 Fig).

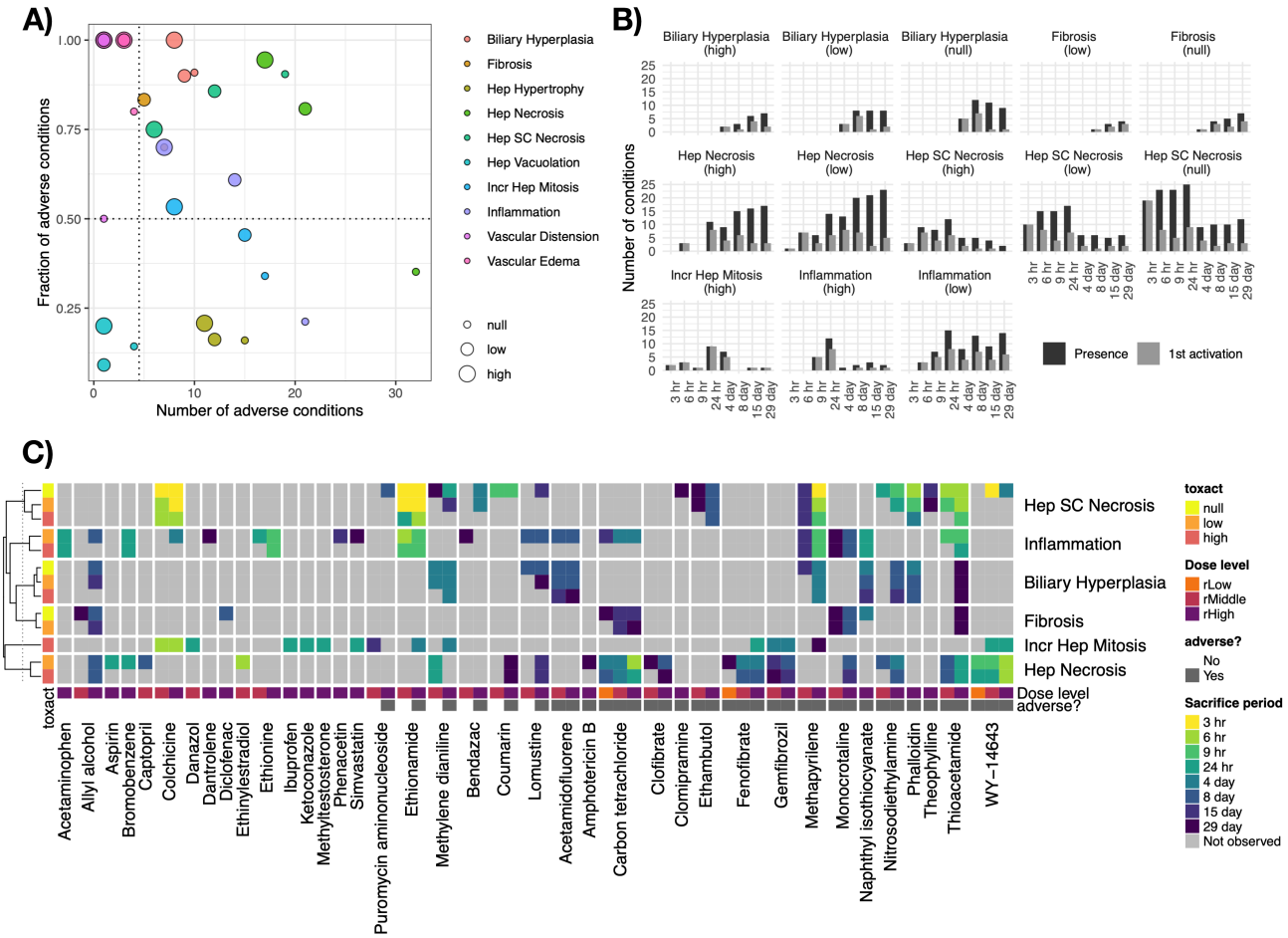

Fig 2: Distribution and relation of histopathological findings across time series. A) Number of occurrences in adverse time series and the fraction of adverse time series among all occurrences of the given finding for all histopathological findings at 3 different toxscore cut-offs, namely “null” (toxscore>0), “low” (toxscore>0.67) and “high” (toxscore>1.34). Histopathological findings, out of which at least 50% and at least 5 of the occurrences were found in adverse conditions timeseries were considered adverse B) Frequency of histopathological findings at different timepoints, as well as the frequency of the respective first activations C) Time of first activation across timeseries labelled as adverse or non-adverse.

Known pathways in DILI preceding adverse histopathology

To identify time-concordant cellular changes preceding later adverse histopathology, we next defined the up- or downregulation TFs or pathways as events and identified 911 significantly enriched (p-value<0.05) pathway-level events (37.3%), and 108 TF-level events (33.6%). The high number of significant events is a result of the overall larger dysregulation observed in adverse time series. We next evaluated time concordance for a set of ten known events in DILI (S3 Table). Recycling of bile acids and salts is the most significantly enriched geneset among the ones linked to known events and overall (Fig 3). Also down-regulation of the other bile acid gene sets is significantly enriched (p-value < 0.05) pointing to an overall down-regulation of bile acid metabolism. While cell death is also only found to be up-regulated, dysregulation in both directions is found to precede injury for all other key events (Fig 3). However, only for peroxisomal processes, namely peroxisomal protein import and beta-oxidation of very long fatty acids, both directions were significantly enriched indicating that dysregulation in either direction might be linked to injury. Overall, significantly enriched gene sets are found for all represented known events in DILI (p-value < 0.05) indicating that our analysis is able to recover known cellular events.

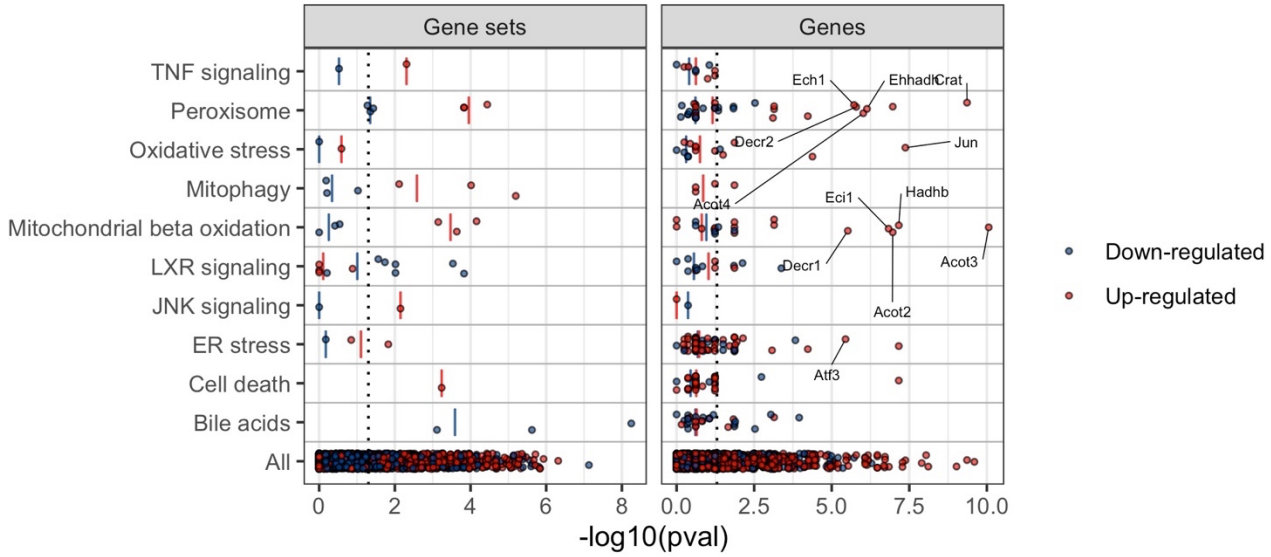

Fig 3: Enrichment of known events in DILI before adverse histopathology based on gene sets as well as individual gene members. The enrichment of first activation before or at adverse histopathology is shown for gene sets mapping to known key events in DILI and genes in these gene sets. Aligning with the expected direction, a significant down-regulation of LXR signalling and bile acid-related pathways is observed, while all other gene sets were found to be more significantly up-regulated. Only for peroxisomal pathways, both directions were significantly enriched indicating that dysregulation in direction might be linked to adverse histopathology. Furthermore, we show which genes show significantly enriched and strong (|logFC|>1) dysregulation providing additional insight into the processes. Among others, Acyl-CoA thioesterase 3 (*Acot3*), which is involved in mitochondrial beta oxidation, is identified as overall most significantly enriched gene.

We next analysed the enrichment of significantly and strongly (|logFC|>1) dysregulated individual genes from the above gene set, with the hypothesis in mind that such genes might be able to provide insight on a more detailed level (S2 File). Among the ten most significantly enriched gene-level events, three are involved in known processes, namely the up-regulation of Acyl-CoA thioesterase 3 (*Acot3*) and Carnitine O-Acetyltransferase (*Crat*) which are involved in mitochondrial and peroxisomal beta oxidation, respectively, as well as the Jun Proto-Oncogene (*Jun*) which plays a role in oxidative stress. All of the other genes among the ten most significantly enriched gene-level events are also involved in mitochondrial and peroxisomal processes except Growth Arrest And DNA Damage-Inducible Protein *Gadd45a* which has a known role in hepatic fibrosis [25]. For JNK signalling, we did not find any significantly enriched genes indicating that while the overall process is changing none of the individual genes shows strong and frequent expression changes. This shows that both gene- and

gene-set level analysis can provide complementary insights into cellular changes preceding DILI, and that in some cases effects can be attributed in individual genes which might give more detailed information about the cellular changes.

While significant enrichment before or at adverse histopathology can be regarded as a necessary criterion for time concordance, the temporal event relationship can be further characterised based on the observed behaviour across experimental conditions which may be useful to further prioritize mechanistically relevant pathways in a hypothesis-free manner. Following the Bradford-Hill considerations, we hypothesize that this might be the case for observed effect size, frequency and specificity of event occurrence before adverse histopathology. Firstly, we investigated how strongly pathways were dysregulated comparing the maximal |logFC| per adverse time-series (Fig 4). High median max. |logFC|s were overall found for mitochondrial and peroxisomal pathways and the highest median max. |logFC| among all significant events was found for mitochondrial fatty acid oxidation of unsaturated fatty acids. At the same time, however, the high variance for pathways with high median max. |logFC| as well as the only moderately high |logFC|s observed for other known pathways in DILI, such as programmed cell death. This indicates that a high magnitude of |logFC| is not necessary to contribute to an adverse event, but at the same time can be a useful property to further prioritize important pathways.

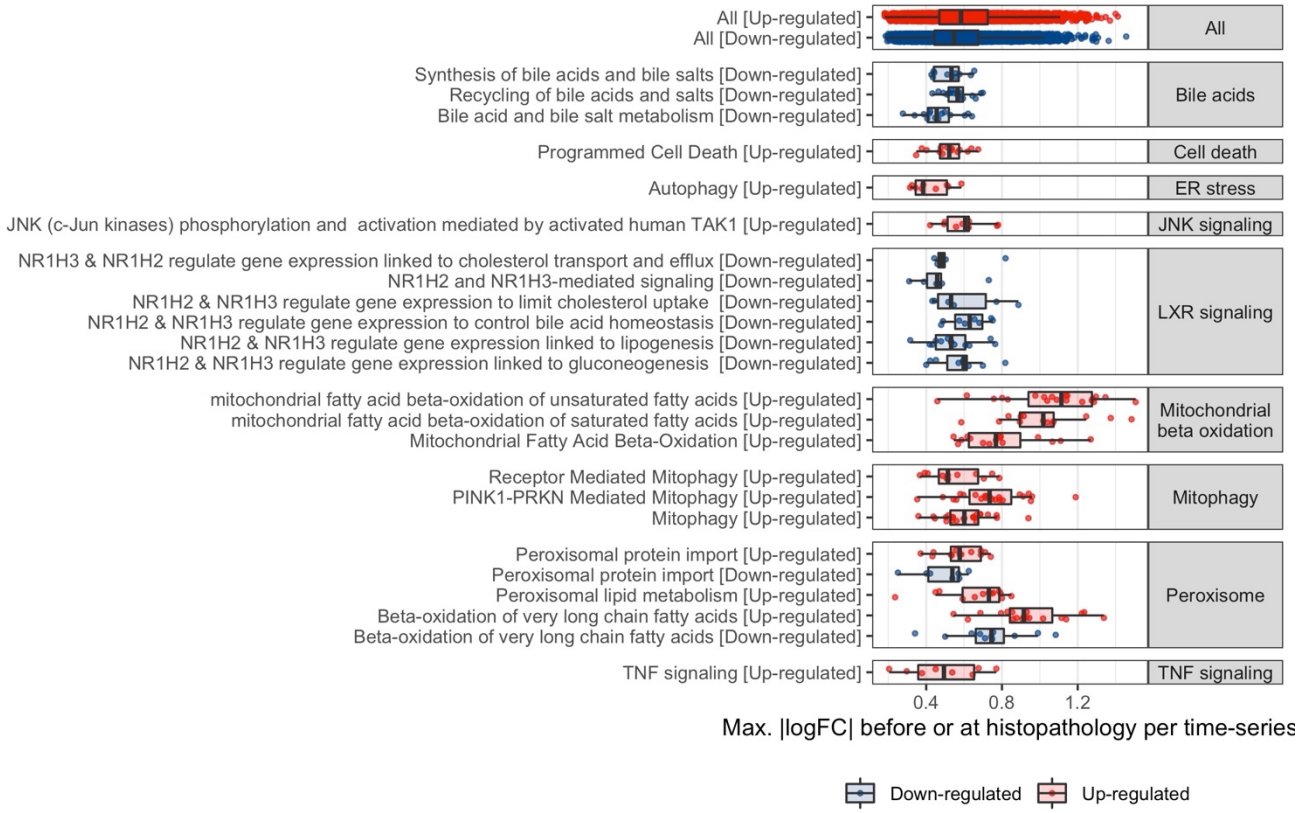

231

232 **Fig 4: Observed max. |logFC| before adverse histopathology.** For known processes in DILI which
233 correspond to significantly enriched events before adverse histopathology, the max |logFC| before
234 adverse histopathology is shown. A high logFC is found for mitochondrial beta oxidation and followed
235 by peroxisomal beta oxidation and mitophagy. As reference, also the background distribution of all
236 max. |logFCs| is shown.

237 We next analysed to what extent dysregulation in a pathway is predictive for a particular type of
238 histopathology. To this end, we calculated across how many adverse time-series each pathway is
239 observed, summarised by the true positive rate (TPR), and the positive predictive value (PPV)
240 indicating whether presence of the key event is a confident indicator for the later adverse event (Fig
241 5). We focus on significantly enriched events only (p-value < 0.05) and find a trade-off with respect to
242 the highest TPR and PPV (Fig 5; for distribution of all events see S3 Fig). This generally shows that
243 either highly frequent events with lower specificity can be identified or more specific events at the
244 expense of lower frequency. Thereby, known events are found at both sides of the spectrum, with
245 increased mitophagy being the most frequent known event (TPR: 0.41, PPV: 0.72) and bile acid
246 recycling the most frequent event among those which are also highly confident (TPR= 0.30, PPV:1).

Surprisingly, lower frequencies are particularly observed for stress response and signaling pathways with only LXR-dependent gene expression linked to lipogenesis reaching a TPR over 20%. We argue that one cause for lower observed frequencies is that these pathways are predominantly and initially mediated through post-transcriptional alterations instead of gene expression changes, making the expression of pathway members a weak proxy for pathway activation in early pathogenesis and explaining the overall low frequencies. In fact, one reason LXR-dependent changes might have achieved higher frequencies as they explicitly include the downstream regulated genes unlike the other signalling and stress response pathways. We hence next investigated the activity of known TFs in DILI preceding adverse histopathology, which might better describe early perturbation response preceding downstream gene expression changes.

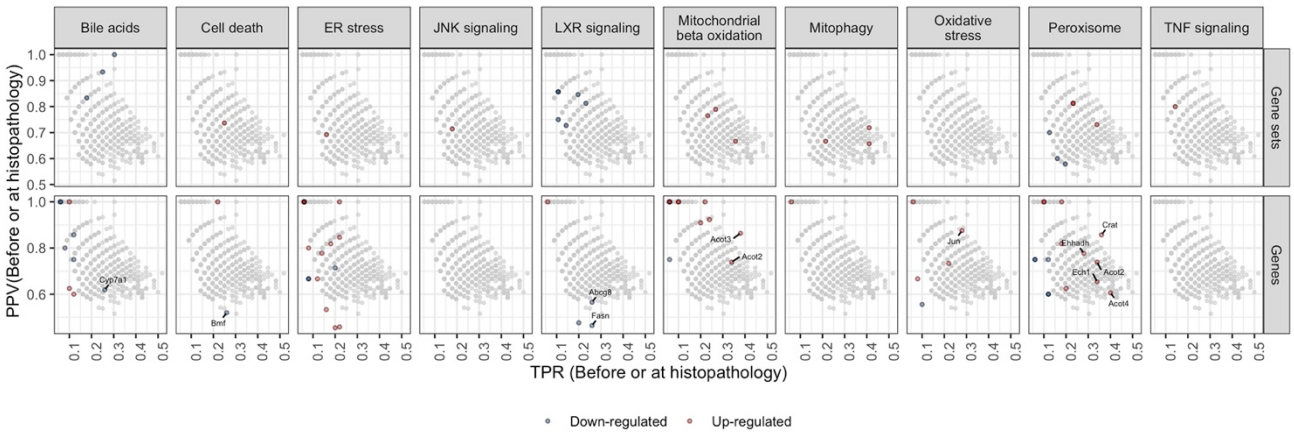

Fig 5: True positive rate (TPR) and positive predictive value (PPV) before or at histopathology of genes and gene sets in known key events in DILI. Events related to the given known key event are shown in red or blue indicating an up- or downregulation, respectively. If the event was over-represented before adverse histopathology (p-value < 0.05) the point was additionally circled in black. The background distribution of all genes or gene sets is shown in grey.

Known TFs in DILI preceding adverse histopathology

To gain insight into signalling and expression regulation preceding adverse histopathology, we next looked into known TFs mediating the stress response and signalling pathways already introduced above, as well as nuclear receptors which take in important roles in liver physiology and malfunctions

and can be, both, MIEs or KEs (mapping shown in Fig 6A). Consistent with the pathway-level results, an enriched up-regulation is found for Nuclear factor erythroid 2-related factor 2 (Nfe2l2) which is a key mediator of oxidative stress [18,26] as well as the Nf-κB subunits Rela and Nfkb1 indicating inflammation [27], while the Oxysterols Receptors LXRα (Nr1h3) and LXRβ (Nr1h2) which control lipid metabolism showed enriched down-regulation [28].

For ER stress, we included three TFs mapping to the three branches of unfolded protein response [29]: Activating transcription factor 4 (Atf4), Activating transcription factor 6 (Atf6) and X-box binding protein 1 (Xbp1). Atf4 up-regulation was found to be most significantly enriched, most frequent and also showing the largest logFC. This highlights its overall importance in mediating ER stress and is consistent with the known role for ATF4 in DILI [30]. While Atf4 is a member of the pro-apoptotic unfolded protein response branch, the ATF6 and XPB1-mediated branches tend to be cytoprotective [31]. In agreement with this, Atf6 was not significantly enriched, however, Xbp1 showed rare but significantly enriched down-regulation.

Transcription Factor AP-1 (Jun) which is one of downstream target TFs of JNK signaling was not significantly enriched in either direction due its rare activation among adverse time series although JNK signaling up-regulation itself was significantly enriched with *Jun* up-regulation being one of the most significantly enriched gene-level events. However, JNK signaling is particularly known in acetaminophen-induced liver injury and in this context leads to hepatocyte death through interactions with Sab on the mitochondrial outer membrane and not through transcriptional regulation mediated by AP-1 [32,33]. As increased Jun activity is hence known to be a consequence of JNK signaling but not a cause of injury, it would be plausible to see enriched pathway activity but not in TF activity before adverse histopathology.

Overall, we were able to show significant enrichment of some of the known TFs in DILI before adverse histopathology and can also biologically reason the absence of significance for others. While none of the included TF-level events ranked as most significant or most strongly changing before adverse

histopathology as in the analysis of pathway-level events, the down-regulation of Nr1h3, which is involved in lipid metabolism, was identified as most frequent event indicating that the linked physiological changes are commonly but not specifically found before injury. Similarly, the up-regulation of stress response, indicated by Nfe2l2 and Atf4, was found to be frequent aligning with their role in adaptive stress response [34]. Overall, frequency might hence be a useful metric to identify pre-adverse cellular events which precede injury but are not highly specific.

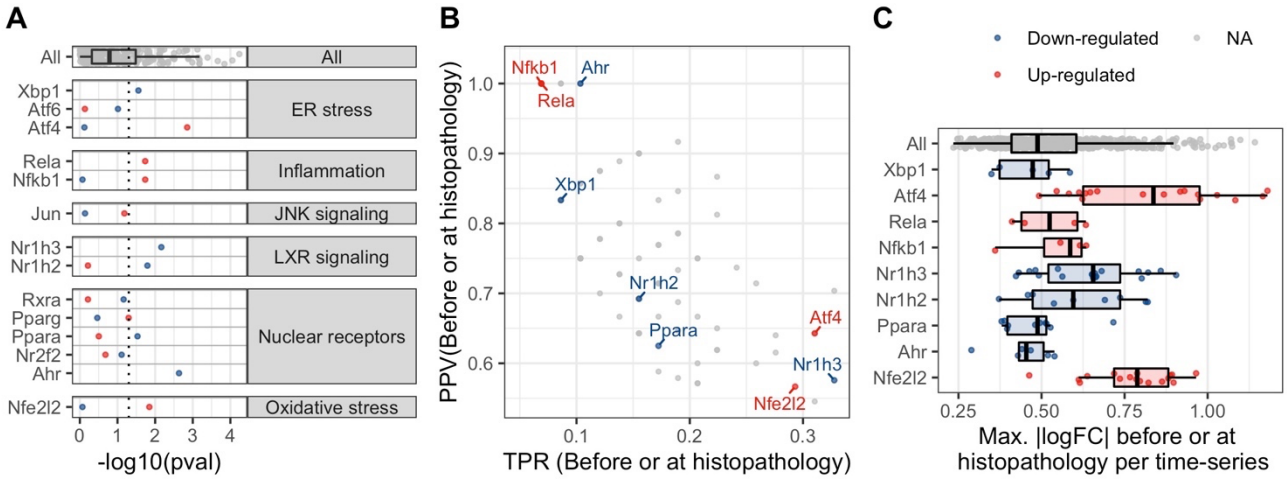

Fig 6: Temporal concordance of nuclear receptors and adaptive response transcription factors (TFs) in DILI. For known TFs in DILI the following time concordance metrics are shown: A) The enrichment significance before or at first adverse histopathology, B) Positive Predictive Value (PPV) and True Positive Rate (TPR), C) Max. mean |logFC| before or at first adverse histopathology.

Data-driven prioritization of cellular events taking place before adverse histopathology

As many events were found to be significantly enriched before adverse histopathology, we next aimed at identifying and characterizing events most supported by time concordance, and hence to move closer to the eventual aim of constructing AOPs from data (All time concordance metrics in S2 File). Among all significant pathway-level events, some known events in DILI ranked highest by enrichment p-value while others rank highest by max. |logFC| before adverse histopathology. In contrast, known TFs in DILI were found as most frequent ones in the dataset. We hence next looked into the top 10

311 TF- and pathway-level events identified using max. |logFC|, the enrichment p-value, and the TPR
312 before or at adverse histopathology. These are shown in Fig 7 and summarised in S4 Table. The next
313 most significantly enriched pathway-level event after decreased bile acid and salt recycling was the
314 down-regulation of glycosaminoglycan metabolism and the most significantly enriched TF-level event
315 was the down-regulation of Transcription factor activating enhancer binding protein 4 (Tfap4) which
316 shows emerging roles in cell fate decisions [35]. Among the up-regulated events, the most significant
317 enrichment is found for cell cycle checkpoints and DNA repair among the pathway-level events as
318 well as E2F Transcription Factor 2 (E2f2), which controls cellular proliferation and liver regeneration
319 [36], among the TF-level events. E2f2 up-regulation was also identified as 2nd most frequent TF event
320 after the down-regulation of Nr1h3 and among the top 10 most strongly changing TF events further
321 highlighting its strong time concordance. The most frequent genesets point to translation regulation
322 via Eukaryotic translation initiation factor 2A (EIF2a) including the upstream response mediated by
323 eIF-2-alpha kinase GCN2 and the downstream role in protein translation mediated through
324 interactions with tRNA. EIF2a is part of the same UPR branch as Atf4 and causes its preferential
325 translation which, among others, mediates autophagy and proapoptotic response [29,37].
326 Furthermore, increased folding of actin by Chaperonin containing tailless complex polypeptide 1
327 (CCT) or tailless complex polypeptide 1 ring complex (TRiC) is found frequently and with large effect
328 size and has been previously linked to proteostasis and autophagy [38,39]. As most strongly
329 dysregulated events, metabolic pathways are found pointing to increased beta oxidation, as well as
330 decreased cholesterol biosynthesis and tyrosine catabolism. Also the Sterol Regulatory Element
331 Binding Transcription Factors Srebf1 and Srebf2 which control cholesterol biosynthesis, as well as
332 Nr1h3 which controls Srebf1 expression are among the most strongly down-regulated TFs. Overall,
333 the derived time concordant events, which take place between the beginning of treatment and onset
334 of adverse histopathology, hence include known and plausible events in liver injury which can be
335 further characterized based on their frequency, significance and logFC.

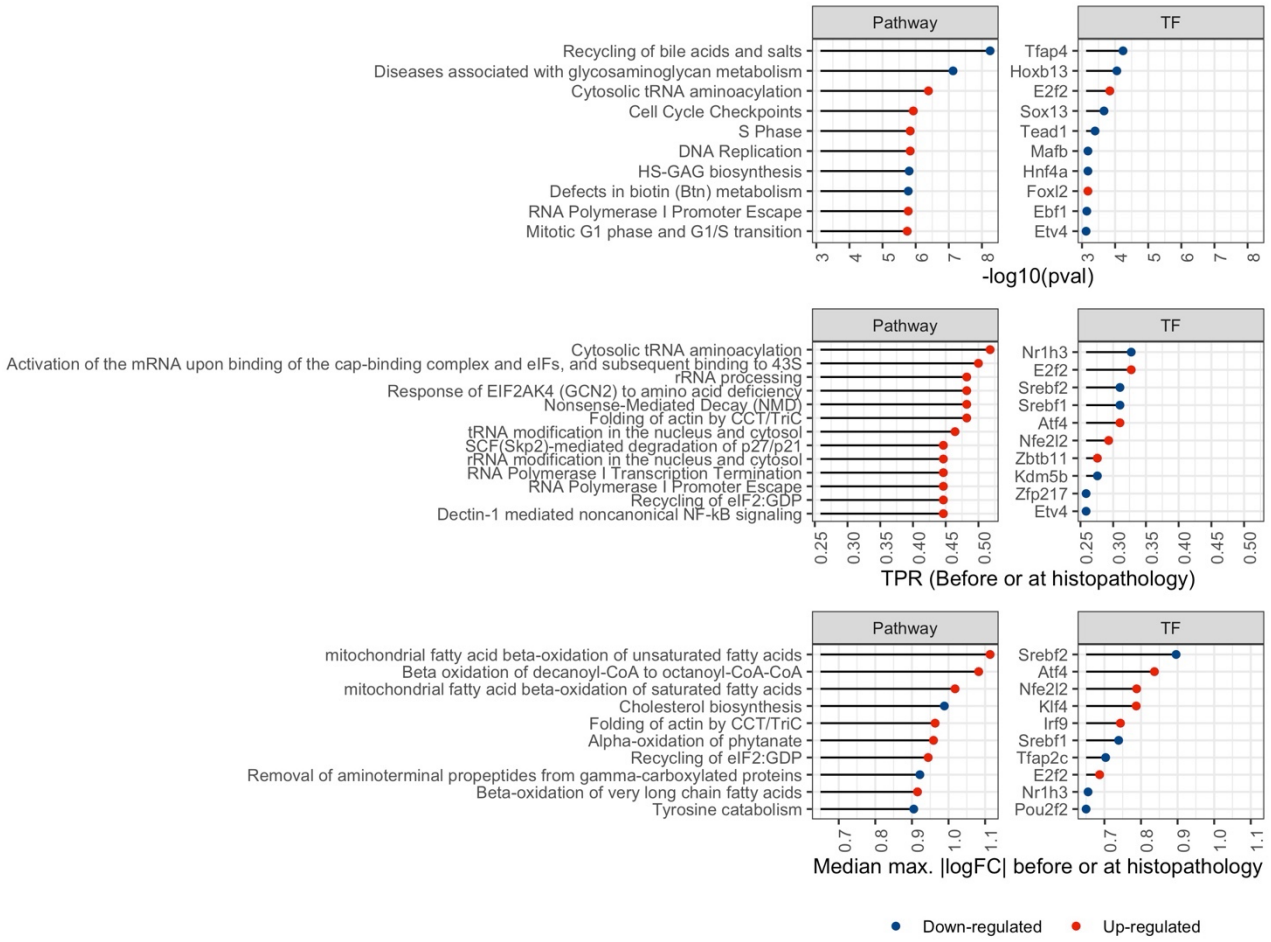

Fig 7: Highest ranking events by time concordance metrics. The 10 transcription factor (TF)- and pathway-level events ranking highest by enrichment p-value, median max. |logFC| and true positive rate (TPR) before or at histopathology is shown.

Identifying mechanistic hypotheses combining known TF functions and time concordance

While both pathways and TFs constitute interpretable events in this study, further prior knowledge is available on how TFs function on a molecular level allowing us to derive more detailed hypothesis. Firstly, TF activity can generally be modulated through changes in expression or in post-transcriptional regulation as consequence of cellular signaling or environmental changes. In case of transcriptional regulation, changes in mRNA levels should precede changes in TF activity estimated based on regulon expression and hence time concordance can be used to gain support for transcriptional TF

regulation. Being only interested in TF events with a potential mechanistic link to liver injury, we studied how significantly concordant expression and activity for each TF are enriched before adverse histopathology (Fig 8A). The strongest evidence for a role in DILI pathogenesis is found for 15 TF events which show both significantly enriched TF expression and regulon activity, providing complementary evidence of TF importance and hinting at transcriptional regulation. While this is not the case for the 77 TF events which only show significantly enriched TF activity, including increased E2f2 or Klf4 activity, this can be explained by post-transcriptional regulation potentially describing earlier response patterns which are a direct consequence of upstream signaling. In contrast, 33 TF events with only significant gene expression, such as increased Jun or Myc, might be already showing changes in expression but not sufficiently large changes in activity yet. As this rather indicates a role in later pathogenesis and expression is only regarded as supporting evidence, these TFs have not been included in downstream analysis.

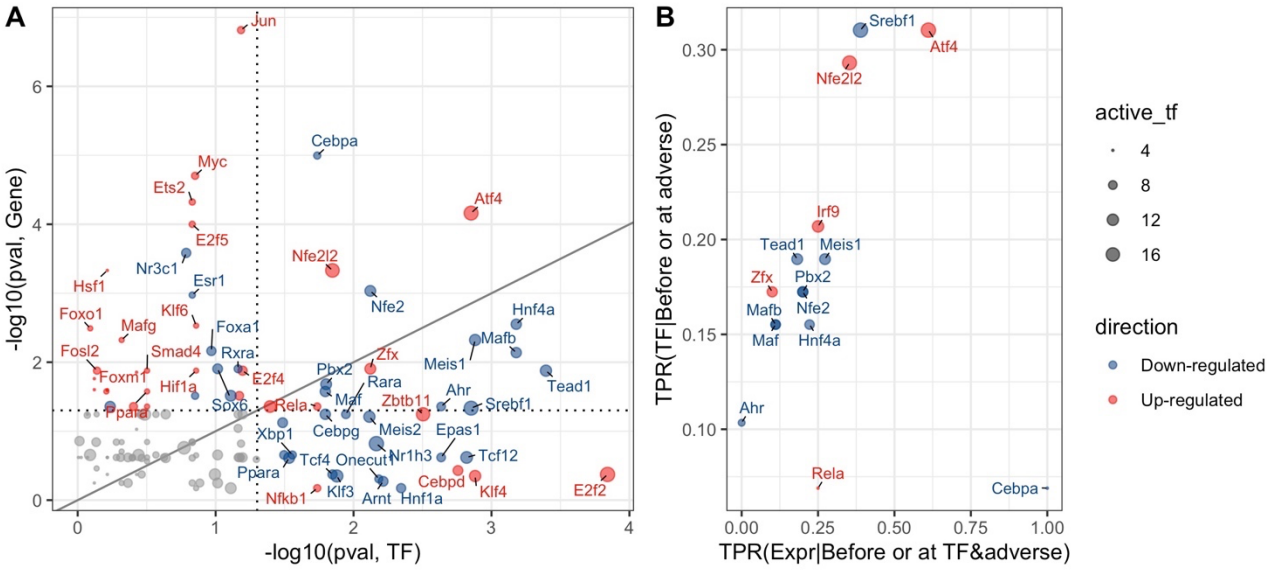

Fig 8: Transcription Factor (TF) activity and expression before adverse histopathology. A) Significance of enrichment in adverse conditions for matched TF activity and expression-based events. Events only found on the expression or TF level are not included in the figure

due to the absence of a statistical test for those. B) For significantly enriched TF activity-based events, the frequency of observing expression before TF activity is shown.

As we have seen in Fig 8A, some TFs show significant enrichment before adverse histopathology, both, on the gene expression and TF activity level. To derive stronger mechanistic evidence for induction we next evaluated how frequently expression changes precede TF activity in the same adverse time-series and compare this against the overall frequency of TF event occurrences preceding adverse histopathology (Fig 8B). Among the events with significant enrichment of TF expression and activity, the most frequent evidence for induction was found for the down-regulation of CCAAT/enhancer-binding protein alpha (Cebpa). In humans, decreased CEBPA expression is not only known across liver diseases, exogenously increased CEBPA expression has also been shown to reverse liver injury and is explored as therapeutic target in hepatocellular carcinoma [40]. The event with the 2nd highest relative frequency of expression preceding TF activity as well as the highest frequency of TF activity preceding injury is ATF4, for which expression is known to be induced as part of the ER stress response contributing to adverse liver phenotypes [41,42]. In contrast, it was found that for the Aryl Hydrogen Receptor, Ahr, changes in expression never preceded those in TF activity providing counterevidence for transcriptional reduction despite significant enrichment of expression changes preceding injury [43].

After investigating the mode of regulation for individual TFs above, we next considered how these TFs are interlinked. To this end, we identified protein-protein interactions and, for induced TFs, TF-target gene interactions between significantly enriched TFs which showed significant enrichment before adverse histopathology for, both, expression and regulon activity as well as evidence of expression preceding TF activity within the same adverse time series. Results of this analysis are shown in Fig 9, and details on the observed absolute and relative frequencies, as well as the source of the interaction are shown in S5 Table. One of the two most frequently identified interaction by absolute frequency is Nr1h3 down-regulation resulting in reduced Srebf1 activity. Furthermore, Srebf1 is also linked to upstream regulation by Nr1h2 which interacts with Peroxisome Proliferator-Activated

Receptor (Ppara) in both directions, and this cross-talk between Ppara and LXR regulating Srebf1 expression has been explicitly studied in the context of fatty acid metabolism regulation [44–46]. The 2nd most frequently observed interaction is the down-regulation of Transcription Factor 12 (Tcf12) inducing reduced activity of TEA Domain Transcription Factor 1 (Tead1). While Tead1 is indeed known to be involved in liver diseases and injury [47,48] , the interaction itself has not been reported before in the context of liver injury and the same applies also for the other upstream Tead1 regulators identified. It should also be noted that for these interactions first activation is only found at the same time but not in the time-concordant order providing weaker evidence than for example the interaction between Nr1h3 and Srebf1. As additional larger TF cluster, decreased activity of the Hepatocyte Nuclear Factor 1 (Hnf1a), Retinoic Acid Receptor alpha (Rara) and Pancreatic And Duodenal Homeobox 1 (Pdx1) was found to lead to decreased expression and activity of Hepatocyte Nuclear Factor 14 (Hnf4a) which is linked to reduced expression and activity of CCAAT/enhancer-binding protein (Cebpa) through edges in both directions. This cluster stands out due to the high confidence score of all interactions except the edge between Pdx1 and Hnf4a indicating that there is strong support based on prior knowledge for the involved interactions. Furthermore, it was previously found that artificially increased expression of Hnf4a is able to reverse hepatic liver failure in rats while also restoring expression of a highly interconnected TF network including Hnf1a and Cebpa which supports the identified interactions [49,50]. One of the yet unknown TFs in DILI is Meis Homeobox 1 (Meis1) which is generally known in a developmental context. However, it's down-regulation in early pathogenesis is supported by enriched TF activity and differential expression before adverse histopathology as well as upstream regulators which are also enriched before adverse histopathology.

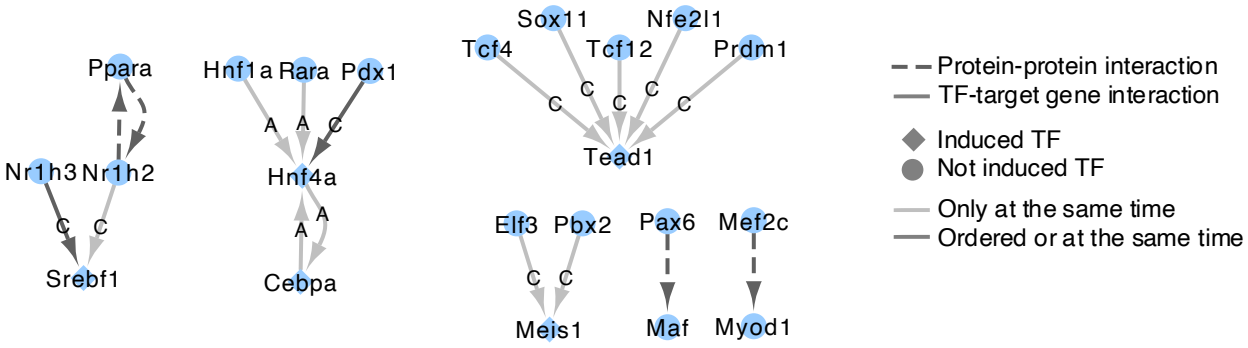

411

412 **Fig 9: Causal relationships between TFs supported by time concordance.** For TFs which are
413 significantly enriched before or at adverse histopathology, known causal relations are shown in which
414 the upstream event is found before or at the downstream event in at least 20% of adverse cases. For
415 induced TFs for which expression is found before regulon activity and significantly enriched, not only
416 protein-protein interactions are considered but also upstream TF-target gene interactions annotated
417 with DoRothEA confidence scores (A: High confidence, C: Medium confidence). Only interactions
418 between down-regulated nodes are found which is indicated by the blue node colour.

419 ## Time-concordant events reflecting disease progression

420 While events do not have to be activated continuously to be causally involved in pathogenesis, events
421 with consistent or increasing activation over time are particularly interesting as biomarkers as they
422 can be experimentally measured without the chance of missing the timepoint of activation, and can
423 potentially reflect disease progression beyond early pathogenesis. We therefore studied which TFs
424 and pathways show time-dependent activation by testing for significant Spearman correlation
425 between activation logFC and time in adverse time-series, and whether this overlaps with the
426 previously derived time concordance (Fig 10). Overall, 118 pathways and 19 TFs were supported by
427 both, significant time concordance and dependence, which represents 86.1% or 70.4% of the time
428 concordant events, and 59.9% or 48.7% of the time-dependent events, respectively.

429 On the pathway level, multiple genesets pointed to a reduced level plasma lipoprotein particle
430 assembly and remodelling indicating changes in lipid distribution. This aligns with the known
431 dyslipidaemia in chronic liver diseases, including decreasing serum values of LDL, HDL, total
432 cholesterol, and triglycerides with increasing severity of disease, based on which previous studies

433 suggested that routine monitoring of lipid profiles can improve the outcome for CLD patients [51].
434 Furthermore, a down-regulation of response to metal ions was found which could be related to
435 metallothioneins which protect against oxidative stress and are able to chelate heavy metals [52].
436 Both directions of dysregulation were previously observed in liver diseases: While a negative
437 correlation with disease progression was found in hepatocellular carcinoma [53], a positive correlation
438 was found in most other liver diseases including acetaminophen-induced liver injury [54]. This
439 indicates that opposite directionality is more plausible based on current literature knowledge, but
440 cannot be fully clarified. The most time-concordant and -dependent TF event was down-regulation of
441 SRY-Box Transcription Factor 13 (Sox13) which is generally involved in cell fate [55] and embryonal
442 development [56] but does not have well understood functions on a more detailed level. In contrast,
443 the next most significant time dependence is found for the hepatocyte nuclear factors Hnf1a and
444 Hnf4a, as well as Cebpa which are known to negatively correlate with liver cirrhosis in rats [57,58].
445 Overall, this shows that a mechanistic role for time-concordant and -dependent events is strongly
446 supported by the understanding of adverse liver phenotypes.

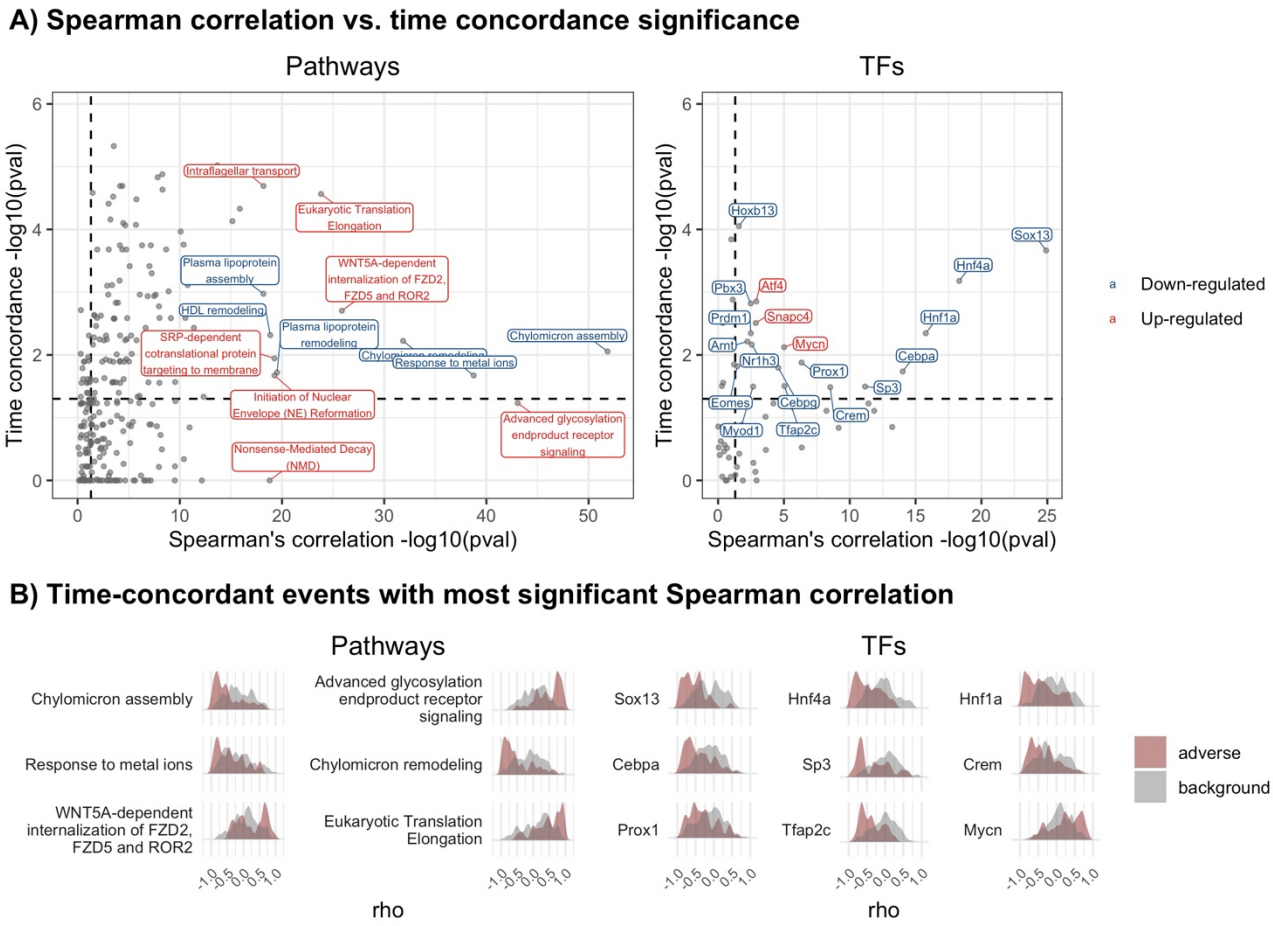

Fig 10: Combining time dependence and concordance to identify mechanistically supported biomarkers. A) The relation between time concordance, quantified by the enrichment p-value for event activation before adverse histopathology, and time dependence, quantified by the meta p-value for Spearman corelation between time and event activation across adverse conditions, is shown. B) For events with the most significant time-dependence, the distribution of correlation coefficients is shown providing further insight into the strength of correlation and consistency across adverse conditions.

While in general events with highly significant time dependence also showed highly significant time concordance, some exceptions were found in which only one of both was highly significant. For instance, the pathway with the 2nd most significant time-dependence (p-value < 10^{44}) is signaling via advanced glycosylation end product receptor (RAGE) which contributes to inflammation and oxidative stress generation and did not pass the significance threshold for time concordance (p-value = 0.058). RAGE expression and activity, which are both induced by binding of RAGE ligands, are thereby known to be up-regulated in various hepatic disorders resulting in a positive feedback loop explaining

462 increasing or sustained RAGE activation [59]. This indicates that, while RAGE signaling is correlated
463 with progression, there is no clear evidence for a role in early pathogenesis preceding adverse
464 histopathological changes. In contrast, SUMOylation of TFs, is time-concordant (p-value = 0.002) but
465 not -dependent (p-value = 0.48) indicating a mechanistic role in early pathogenesis which is not
466 sustained over time. This aligns with the finely regulated and pleiotropic roles of SUMOylation in post-
467 transcriptional regulation which have also been found to be involved in the context of liver diseases
468 [60].

469 Limitations of this study

470 In this study, we introduce a time-concordance based approach to derive mechanistic insight from
471 gene expression and histopathology data. We are able to recover known mechanisms in DILI as well
472 as able to propose novel and detailed mechanistic hypotheses. However, the presented analysis only
473 describes event cascades in the TG-GATEs dataset and hence is based on a limited number time-
474 series as well as only few timepoints within each time-series. This does not only mean that rare events
475 might be missed in the measurements and that small effects might not be identified as significant, but
476 also that there is potentially a bias based on the tested compounds towards the represented modes
477 of toxicity.

478 Furthermore, the analysis is limited by how confidently biological processes are inferred from the data.
479 This was for instance demonstrated by the differences between pathway and TF activation for
480 signalling and stress response pathways highlighting the discrepancy between protein activation and
481 gene expression. As only pathways induced through changes in gene expression or their downstream
482 expression footprints [61] can be confidently detected, this means that good estimates of time
483 concordance can predominantly be derived for intermediate or later key events while earlier key
484 events or molecular initiating events, such as drug metabolism, cannot be estimated based on the

485 data. That being said, this is a limitation of gene expression data in general and the time concordance
486 approach would also be able to integrate other data types describing events not covered yet.

487 Moreover, multiple choices were made to align our analysis to the AOP concept prioritizing
488 mechanisms supported by prior knowledge over purely data-driven hypothesis. First, detailed insights
489 might be lost by summarising results to the pathway level. While generally measurements for
490 individual genes can be noisy, this can be summarised in different ways e.g. based on similarity in
491 expression profiles [15]. In this study, however, we used curated gene sets due to their interpretability
492 and to derive modular events as defined in the AOP framework. Additionally, prior knowledge was
493 taken as ground truth, both in the gene set and interaction analysis, meaning that only generally
494 known pathways and interactions can be discovered. Like all methods based on curated gene set and
495 interactions, it is hence informed and biased by the current understanding of biology. However, this
496 prior biological knowledge contributes to the biological plausibility of the derived events and
497 relationships contributing to the weight of evidence of our findings in the context of AOPs.

498 Conclusion

499 In this study, we introduce first activation as concept to quantify the strength of temporal concordance
500 between events across time series. With this approach, we study gene expression-based TF and
501 pathway-level events found before adverse histopathology indicating liver injury in repeat-dose
502 studies in rats from TG-GATEs as a case study. We find some known processes in DILI to be highly
503 confident, e.g. bile acid recycling, while others are highly frequent but less specific including adaptive
504 response pathways. Here, the eIF2α/ATF4 pathway as eiF2α and Atf4 are identified as most frequent
505 pathway and TF, pointing to an important role of eIF2α/ATF4-mediated stress response [37].

506 Beyond quantifying time concordance for known and potentially novel events in DILI, we additionally
507 show how time concordance can be combined with prior biological knowledge to generate hypothesis
508 on potentially causal gene-regulatory cascades in DILI. Amongst others, this identifies LXRα down-

509 regulation leading to decreased Srebf1 expression, an interaction known to regulate fatty acid
510 synthesis in the liver [28], but also characterizes yet unknown TFs based on their time concordance,
511 their mode of regulation (either transcriptional or post-transcriptional) and potential upstream
512 regulators and downstream effectors. One of the identified induced TFs is Meis1 which is supported
513 by significantly enriched decrease in expression and activity before adverse histopathology, as well
514 as upstream regulators which also show significant enrichment of regulon activity and are found within
515 the same time series. On top of time concordance, we also derive each event's time dependence and
516 show that events mechanistically involved in early pathogenesis do not necessarily reflect disease
517 progression and vice versa. However, for some events, e.g. Sox13, both properties are found and
518 these may be useful biomarkers which reflect injury progression and already change preceding
519 histopathological manifestation.

520 We believe that the described analysis can provide supporting evidence for mechanistic links between
521 events in line with the evolved Bradford-Hill considerations and can hence e.g. support AOP
522 development. Furthermore, the approach is not limited to a particular adverse event and can instead
523 quantify the interaction between any two events represented in time series in a data-driven and
524 automatable fashion. We make the results of our analysis on the TG-GATEs *in vivo* liver data publicly
525 available in a Shiny app through which users can query the most time-concordant events for more
526 specific types of histopathology and study in detail in which time series time concordance was
527 observed or not observed (https://github.com/anikaliu/DILICascades_App).

528 Methods

529 Open TG-GATES data processing

530 The TG-GATES gene expression data from repeat-dose studies in rats was downloaded from the Life
531 Science Data Archive (DOI: 10.18908/lsdba.nbdc00954-01-000). The raw liver gene expression

levels were background corrected, $\log_2$ transformed, and quantile normalized with the rma function of the affy package per treatment across all doses and timepoints [62]. Quality control was then performed using the ArrayQualityMetrics package [63] and detected outliers with high distance to other experiments or unusual signal distribution were removed (List of removed outliers summarised in S1 File). The platform information for the Affymetrix Rat Genome 230 2.0 Array was derived from Gene Expression Omnibus [64] (GEO accession: GPL1355) and was then used to summarise probe IDs to rat gene symbols by median for all probes mapping uniquely to one gene symbol. Only compound-dose combinations with at least 5 measured timepoints after quality control were included.

Definition of adverse histopathology

To characterize the extend of histological findings, we used the toxscores by Sutherland et al. [15] in order to consider both severity and frequency of events in a single numerical output measure. These are based on the lesion severity per animal which was first converted to a numerical scale (normal = 0, minimal = 1, slight = 2, moderate = 3, marked or severe = 4) and then summarised across all biological replicates by mean as an aggregate measure for lesion frequency and severity. One characteristic of this measure is that the overall distributions varied between different findings, e.g. inflammation was more frequently annotated with low than with high toxscores while a more balanced distribution of scores was observed for Hepatocellular single cell necrosis (S1 Fig).

To study which histological findings were enriched in adverse conditions, we first defined binary histopathology labels describing the presence of histological findings with different extents in each time-series. Based on the toxscore ranges used by Sutherland et al., three toxscore cut-offs are implemented to describe each histopathological finding “Null” (toxscore > 0), “low” (toxscore > 0.67) and “high” (toxscore > 1.34). We then studied which labels were over-represented in adverse time-series. These were defined using the annotation of Sutherland et al., where pathologists classified compound-dose combinations in the TG-GATEs database as adverse or non-adverse after 4 and 29

556 days of treatment. We used the 29 days classification to define 40 adverse time series and only
557 regarded time-series as non-adverse for compounds which were not classified as adverse at any
558 dose in the negative control, in order to account for the fact that some of the cellular changes of
559 interest might already take place at lower doses, although the resulting phenotype is not considered
560 adverse yet. Out of the 24 compounds represented in adverse time-series, 14 have additionally been
561 classified as hepatotoxic in DILIst and 5 are classified as vMost-DILI-Concern in DILIrank (S2 Table).

562 We defined findings as adverse histopathology if they are observed in at least 5 out of 40 adverse
563 time-series to remove rare histopathological findings, and additionally require that at least 50% of
564 findings are in adverse conditions to remove findings which are unspecific. All labels which were
565 identified with these criteria are significantly enriched using a hypergeometric test (p-value > 0.0001),
566 however, this combination of additional criteria was chosen to exclude findings which are rare or
567 weakly associated.

568 Pathway and TF activity inference

569 The activity of pathways and TFs was derived for each compound based on the expression of its gene
570 sets members using GSVA [65] using a Gaussian kernel and requiring at least 5 genes per gene set.
571 As prior knowledge, we used pathway maps from Reactome [66] which were derived through MSigDB
572 [67] and the msigdbr package [68]. TF activity gene sets were derived from DoRothEA [69] and
573 mapped from human to rat gene symbols with biomaRt [70]. These gene sets describe known,
574 functional TF-gene interactions and are assigned a confidence level based on the strength of
575 evidence of these interactions. Thereby, only the 207 TFs with a high to medium confidence level of
576 A-C were included and the few TF-gene interactions with a negative mode of regulation were removed
577 to better infer TF directionality. To evaluate which pathway or TF is dysregulated, we computed the
578 differential activity in comparison to the time-, vehicle-, and experiment-matched control group using
579 limma [71] and identify significantly dysregulated gene sets (FDR<0.05).

Temporal concordance of events

In this study, the order of events was derived based on each event's timepoint of first activation within each time-series (Fig 1A). For pathways and TFs, we defined first activation as the earliest time of measurement at which significant differential regulation was observed (FDR < 0.05) in each direction, while an additional logFC cut-off has been implemented for individual genes. As first evidence of adverse morphological changes in the liver, we used the first timepoint any of the adverse histopathology label derived before were found.

We were then generally interested in events of interest ***A*** which are first activated before or at the same time as an anchoring event ***B*** and used multiple metrics to quantify the degree of time concordance which can be related to the original work by Bradford Hill (Table 1). Thereby, the key anchoring event in this study was adverse histopathology but we used a more general notation ***B*** as some of the following criteria to quantify time concordance are also applied in the TF analysis where gene expression-derived events are used as anchoring event. First, we used the true positive rate (TPR) which describes how frequently ***A*** is observed before ***B*** among all time-series with ***B*** and hence its consistency across compounds. Thereby, the reported TPR only included time-series for which any event of the same type as ***A***, e.g. TF or pathway, was observed before or at ***B***. Secondly, we use the maximal effect size of ***A*** observed before ***B***, summarised across time-series by median, to characterise the strength of association. To evaluate the significance of the findings, we additionally defined a set of background time-series unrelated to ***B*** (Fig 1B). For adverse histopathology, these unrelated background time-series were the 133 time-series without any observed histological changes***.*** We then computed the enrichment of ***A*** before or at ***B*** using a hypergeometric test and positive predictive value (PPV) of ***A*** for ***B*** which describes how likely ***B*** is observed at the same or a later time given the observation of ***A.***

603 **Table 1: Metrics quantifying the time concordance between a potential preceding event *A* and**
604 **potential later event *B,* and their relation to the original Bradford Hill (BH) considerations.**

BH consideration	Metric	Formula	Description
Consistency	True positive rate (TPR)	p(***A*** →***B***|***B***)	Fraction of time series with event ***A*** with specified temporal relation among time series with event ***B***
Specificity	Positive predictive value (PPV)	p(***A***→ ***B***|***A***)	Fraction of time series with event ***B*** with specified temporal relation among time series with event ***A***
Temporality	p-value	One-sided Fisher's Exact test	Likelihood of observing event ***A*** and ***B*** with specified temporal relation with equal or higher frequency by chance assuming a hypergeometric distribution.
Strength	Effect size in time series with ***B***	Median (logFC)	Median logFC of ***A*** observed in time-series with ***B*** (in comparison to vehicle control)

605 ## Combining time concordance on TF-TF interactions

606 We used 3 sources of causal prior knowledge to derive mechanistic hypotheses linking TFs: Protein-
607 protein interaction between TFs derived from Omnipath through OmnipathR [72,73], TF-target gene
608 interactions from DoRothEA [69] and the link between gene expression and protein levels following
609 the central dogma of molecular biology. Using these interactions as backbone, we then derived those
610 additionally supported by time concordance. Thereby, the dysregulation of the nodes was required to
611 match the reported mode of regulation (edge sign) and the source node or upstream event was
612 required to be observed in at least 20% of cases before or at the same time as the target node or
613 downstream event. For induced TFs, significant enrichment of gene expression (|logFC|>0.5) and TF
614 activity before adverse histopathology was required as well as evidence for changes in expression
615 preceding changes in the same direction in regulon activity within the same time series.

616 ## Time dependence

617 In each adverse time-series, we tested for Spearman correlation between timepoint and event
618 activation logFC using the correlation R package [74], and include a logFC of 0 at timepoint 0 h
619 assuming that there are no differences in comparison to the control group before treatment. We then

identify pathways and TFs which only show significant Spearman correlation in one direction, positive or negative. For those events, we apply the Fisher's combined probability test using the metap R package [75] across all adverse time-series to evaluate whether overall significant correlation between event activation and time is found.

Supporting information

S1 Table. Comparison of quantitative Adverse Outcome Pathway (qAOP) models. Comparison of the first activation concept and other qAOP models with respect to their potential roles in AOP development.

S2 Table. Compounds classified as adverse based on histopathology and concordance with labels from DILIRank and DILIst describing liver side effects observed in humans derived from post-marketing data.

S3 Table. Time concordance metrics for Reactome pathway maps which map to known key events based on literature review.

S4 Table. Time concordance metrics for top 10 ranking events by True Positive Rate (TPR), significance and median max. |logFC|.

S5 Table. TF-TF relations supported by known relations and time concordance. For TF events which are significantly enriched before or at adverse histopathology, known interactions supported by time concordance are shown. With respect to the interaction, the absolute and relative frequency are shown for how often the source TF was observed "before" or "before or at" downstream TF activity. Additionally, the source of the interactions provided in Omnipath are shown for protein-protein interactions and the DoRothEA confidence level for TF-target gene interactions.

S1 Fig. Distribution of toxscores across histopathological findings.

S2 Fig. Frequency of histopathological findings before and after first adverse histopathology. For adverse and non-adverse histopathological findings the frequency before or at first non-adverse histopathology is shown (left). For adverse findings, this indicates how frequently they were one of the first adverse histopathological findings given that they cannot occur before by definition. This identifies single-cell necrosis at any severity ("null"), as the most frequent finding, both in absolute and relative terms.

S3 Fig. Background distribution of temporal association metrics across events. The dependency between different metrics based on the confusion matrix is shown. Hypergeometric tests to identify events which are significantly enriched before adverse histopathology in comparison to non-adverse control time series derive low p-values for events with high TPR and high PPV. Given a number of event activations in non-adverse control time series, there is a monotonous relationship

654 between PPV and TPR with increasing PPV at lower event frequency in non-adverse control time
655 series.

656 **S1 File. Removed outlier samples.**

657 **S2 File. Time concordance metrics for all TFs, pathways as well as genes using both a minimal**
658 **|logFC| of 0.5 and 1.**

659 References

660 1. Hwang TJ, Carpenter D, Lauffenburger JC, Wang B, Franklin JM, Kesselheim AS. Failure of
661 investigational drugs in late-stage clinical development and publication of trial results. JAMA
662 Internal Medicine. 2016;176: 1826–1833. doi:10.1001/jamainternmed.2016.6008

663 2. Harrison RK. Phase II and phase III failures: 2013-2015. Nature Reviews Drug Discovery.
664 2016;15: 817–818. doi:10.1038/nrd.2016.184

665 3. Bai JPF, Abernethy DR. Systems Pharmacology to Predict Drug Toxicity: Integration Across
666 Levels of Biological Organization *. 2012 [cited 5 Jun 2019]. doi:10.1146/annurev-pharmtox-
667 011112-140248

668 4. Leist M, Ghallab A, Graepel R, Marchan R, Hassan R, Bennekou SH, et al. Adverse outcome
669 pathways: opportunities, limitations and open questions. Archives of Toxicology. 2017;91:
670 3477–3505. doi:10.1007/s00204-017-2045-3

671 5. Ankley GT, Bennett RS, Erickson RJ, Hoff DJ, Hornung MW, Johnson RD, et al. Adverse
672 outcome pathways: A conceptual framework to support ecotoxicology research and risk
673 assessment. Environmental Toxicology and Chemistry Wiley Blackwell; Mar 1, 2010 pp. 730–
674 741. doi:10.1002/etc.34

675 6. OECD (Organisation for Economic Co-operation and Development). USERS' HANDBOOK
676 SUPPLEMENT TO THE GUIDANCE DOCUMENT FOR DEVELOPING AND ASSESSING

677 AOPs. OECD Environment, Health and Safety Publications Series on Testing and Assessment.
678 2018; 1–62.

679 7. Hill AB. The Environment and Disease: Association or Causation? Proceedings of the Royal
680 Society of Medicine. 1965; 295–300.

681 8. Meek ME, Palermo CM, Bachman AN, North CM, Lewis RJ, Meek B, et al. Mode of action
682 human relevance (species concordance) framework: Evolution of the Bradford Hill
683 considerations and comparative analysis of weight of evidence. Journal of Applied Toxicology
684 John Wiley and Sons Ltd; 2014 pp. 595–606. doi:10.1002/jat.2984

685 9. Oki NO, Nelms MD, Bell SM, Mortensen HM, Edwards SW. Accelerating Adverse Outcome
686 Pathway Development Using Publicly Available Data Sources. Current Environmental Health
687 Reports. 2016;3: 53–63. doi:10.1007/s40572-016-0079-y

688 10. Oki NO, Edwards SW. An integrative data mining approach to identifying adverse outcome
689 pathway signatures. Toxicology. 2016;350–352: 49–61. doi:10.1016/J.TOX.2016.04.004

690 11. Bell SM, Angrish MM, Wood CE, Edwards SW. Integrating publicly available data to generate
691 computationally predicted adverse outcome pathways for fatty liver. Toxicological Sciences.
692 2016;150: 510–520. doi:10.1093/toxsci/kfw017

693 12. Burgoon LD, Angrish M, Garcia-Reyero N, Pollesch N, Zupanic A, Perkins E. Predicting the
694 Probability that a Chemical Causes Steatosis Using Adverse Outcome Pathway Bayesian
695 Networks (AOPBNs). Risk Analysis. 2020;40: 512–523. doi:10.1111/risa.13423

696 13. Jeong J, Garcia-Reyero N, Burgoon L, Perkins E, Park T, Kim C, et al. Development of Adverse
697 Outcome Pathway for PPARγAntagonism Leading to Pulmonary Fibrosis and Chemical
698 Selection for Its Validation: ToxCast Database and a Deep Learning Artificial Neural Network

699 Model-Based Approach. Chemical Research in Toxicology. 2019;32: 1212–1222.
700 doi:10.1021/acs.chemrestox.9b00040

701 14. Kohonen P, Parkkinen JA, Willighagen EL, Ceder R, Wennerberg K, Kaski S, et al. A
702 transcriptomics data-driven gene space accurately predicts liver cytopathology and drug-
703 induced liver injury. Nature Communications. 2017;8. doi:10.1038/ncomms15932

704 15. Sutherland JJ, Webster YW, Willy JA, Searfoss GH, Goldstein KM, Irizarry AR, et al.
705 Toxicogenomic module associations with pathogenesis: A network-based approach to
706 understanding drug toxicity. Pharmacogenomics Journal. 2018;18: 377–390.
707 doi:10.1038/tpj.2017.17

708 16. Souza TM, Kleinjans JCS, Jennen DGJ. Dose and Time Dependencies in Stress Pathway
709 Responses during Chemical Exposure: Novel Insights from Gene Regulatory Networks.
710 Frontiers in Genetics. 2017;8: 142–142. doi:10.3389/fgene.2017.00142

711 17. Rooney J, Hill T, Qin C, Sistare FD, Christopher Corton J. Adverse outcome pathway-driven
712 identification of rat liver tumorigens in short-term assays. Toxicology and Applied
713 Pharmacology. 2018;356: 99–113. doi:10.1016/j.taap.2018.07.023

714 18. Rooney J, Oshida K, Vasani N, Vallanat B, Ryan N, Chorley BN, et al. Activation of Nrf2 in the
715 liver is associated with stress resistance mediated by suppression of the growth hormone-
716 regulated STAT5b transcription factor. PLoS ONE. 2018;13.
717 doi:10.1371/journal.pone.0200004

718 19. Aguayo-Orozco A, Bois FY, Brunak S, Taboureau O. Analysis of Time-Series Gene Expression
719 Data to Explore Mechanisms of Chemical-Induced Hepatic Steatosis Toxicity. Frontiers in
720 Genetics. 2018;9: 396. doi:10.3389/fgene.2018.00396

721 20. Zhang JD, Berntenis N, Roth A, Ebeling M. Data mining reveals a network of early-response
722 genes as a consensus signature of drug-induced in vitro and in vivo toxicity.
723 Pharmacogenomics Journal. 2014;14: 208–216. doi:10.1038/tpj.2013.39

724 21. Zgheib E, Gao W, Limonciel A, Aladjov H, Yang H, Tebby C, et al. Application of three
725 approaches for quantitative AOP development to renal toxicity. Computational Toxicology.
726 2019;11: 1–13. doi:10.1016/J.COMTOX.2019.02.001

727 22. Hassan I, El-Masri H, Kosian PA, Ford J, Degitz SJ, Gilbert ME. Neurodevelopment and
728 Thyroid Hormone Synthesis Inhibition in the Rat: Quantitative Understanding Within the
729 Adverse Outcome Pathway Framework. Toxicological Sciences. 2017;160: 57–73.
730 doi:10.1093/TOXSCI/KFX163

731 23. Spinu N, Cronin MTD, Enoch SJ, Madden JC, Worth AP. Quantitative adverse outcome
732 pathway (qAOP) models for toxicity prediction. Archives of Toxicology. Springer; 2020. pp.
733 1497–1510. doi:10.1007/s00204-020-02774-7

734 24. Andrade RJ, Chalasani N, Björnsson ES, Suzuki A, Kullak-Ublick GA, Watkins PB, et al. Drug-
735 induced liver injury. Nature Reviews Disease Primers. 2019;5: 1–22. doi:10.1038/s41572-019-
736 0105-0

737 25. Hong L, Sun QF, Xu TY, Wu YH, Zhang H, Fu RQ, et al. New role and molecular mechanism
738 of Gadd45a in hepatic Fibrosis. World Journal of Gastroenterology. 2016;22: 2779–2788.
739 doi:10.3748/wjg.v22.i9.2779

740 26. Copple IM, Goldring CE, Jenkins RE, Chia AJL, Randle LE, Hayes JD, et al. The hepatotoxic
741 metabolite of acetaminophen directly activates the Keap1-Nrf2 cell defense system.
742 Hepatology. 2008;48: 1292–1301. doi:10.1002/hep.22472

743 27. Luedde T, Schwabe RF. NF-κB in the liver-linking injury, fibrosis and hepatocellular carcinoma.
744 Nature Reviews Gastroenterology and Hepatology. NIH Public Access; 2011. pp. 108–118.
745 doi:10.1038/nrgastro.2010.213

746 28. Schultz JR, Tu H, Luk A, Repa JJ, Medina JC, Li L, et al. Role of LXRs in control of lipogenesis.
747 Genes and Development. 2000;14: 2831–2838. doi:10.1101/gad.850400

748 29. Hetz C, Zhang K, Kaufman RJ. Mechanisms, regulation and functions of the unfolded protein
749 response. Nature Reviews Molecular Cell Biology. Nature Research; 2020. pp. 421–438.
750 doi:10.1038/s41580-020-0250-z

751 30. Wijaya LS, Trairatphisan P, Gabor A, Niemeijer M, Keet J, Alcalà Morera A, et al. Integration
752 of temporal single cell cellular stress response activity with logic-ODE modeling reveals
753 activation of ATF4-CHOP axis as a critical predictor of drug-induced liver injury. Biochemical
754 Pharmacology. 2021;190: 114591. doi:10.1016/j.bcp.2021.114591

755 31. Fredriksson L, Wink S, Herpers B, Benedetti G, Hadi M, de Bont H, et al. Drug-induced
756 endoplasmic reticulum and oxidative stress responses independently sensitize toward TNFα-
757 mediated hepatotoxicity. Toxicological Sciences. 2014;140: 144–159.
758 doi:10.1093/toxsci/kfu072

759 32. Seki E, Brenner DA, Karin M. A liver full of JNK: Signaling in regulation of cell function and
760 disease pathogenesis, and clinical approaches. Gastroenterology. 2012;143: 307–320.
761 doi:10.1053/j.gastro.2012.06.004

762 33. Win S, Than TA, Zhang J, Oo C, Min RWM, Kaplowitz N. New insights into the role and
763 mechanism of c-Jun-N-terminal kinase signaling in the pathobiology of liver diseases.
764 Hepatology. John Wiley and Sons Inc.; 2018. pp. 2013–2024. doi:10.1002/hep.29689

765 34. Simmons SO, Fan C-Y, Ramabhadran R. Cellular Stress Response Pathway System as a
766 Sentinel Ensemble in Toxicological Screening. Toxicological Sciences. 2009;111: 202–225.
767 doi:10.1093/TOXSCI/KFP140

768 35. Wong MMK, Joyson SM, Hermeking H, Chiu SK. Transcription factor AP4 mediates cell fate
769 decisions: To divide, age, or die. Cancers. MDPI AG; 2021. pp. 1–15.
770 doi:10.3390/cancers13040676

771 36. Delgado I, Fresnedo O, Iglesias A, Rueda Y, Syn WK, Zubiaga AM, et al. A role for transcription
772 factor E2F2 in hepatocyte proliferation and timely liver regeneration. American Journal of
773 Physiology - Gastrointestinal and Liver Physiology. 2011;301. doi:10.1152/ajpgi.00481.2010

774 37. B'Chir W, Maurin AC, Carraro V, Averous J, Jousse C, Muranishi Y, et al. The eIF2α/ATF4
775 pathway is essential for stress-induced autophagy gene expression. Nucleic Acids Research.
776 2013;41: 7683–7699. doi:10.1093/nar/gkt563

777 38. Pavel M, Imarisio S, Menzies FM, Jimenez-Sanchez M, Siddiqi FH, Wu X, et al. CCT complex
778 restricts neuropathogenic protein aggregation via autophagy. Nature Communications. 2016;7:
779 1–18. doi:10.1038/ncomms13821

780 39. Grantham J. The Molecular Chaperone CCT/TRiC: An Essential Component of Proteostasis
781 and a Potential Modulator of Protein Aggregation. Frontiers in Genetics. Frontiers Media S.A.;
782 2020. doi:10.3389/fgene.2020.00172

783 40. Reebye V, Huang KW, Lin V, Jarvis S, Cutilas P, Dorman S, et al. Gene activation of CEBPA
784 using saRNA: Preclinical studies of the first in human saRNA drug candidate for liver cancer.
785 Oncogene. 2018;37: 3216–3228. doi:10.1038/s41388-018-0126-2

786 41. Fusakio ME, Willy JA, Wang Y, Mirek ET, Baghdadi RJTA, Adams CM, et al. Transcription
787 factor ATF4 directs basal and stress-induced gene expression in the unfolded protein response

and cholesterol metabolism in the liver. Molecular Biology of the Cell. 2016;27: 1536–1551. doi:10.1091/mbc.E16-01-0039

42. Hao L, Zhong W, Dong H, Guo W, Sun X, Zhang W, et al. ATF4 activation promotes hepatic mitochondrial dysfunction by repressing NRF1-TFAM signalling in alcoholic steatohepatitis. Gut. 2020 [cited 6 May 2021]. doi:10.1136/gutjnl-2020-321548

43. Larigot L, Juricek L, Dairou J, Coumoul X. AhR signaling pathways and regulatory functions. Biochimie Open. 2018;7: 1–9. doi:10.1016/J.BIOPEN.2018.05.001

44. Yoshikawa T, Ide T, Shimano H, Yahagi N, Amemiya-Kudo M, Matsuzaka T, et al. Cross-talk between peroxisome proliferator-activated receptor (PPAR) α and liver X receptor (LXR) in nutritional regulation of fatty acid metabolism. I. PPARS suppress sterol regulatory element binding protein-1c promoter through inhibition of LXR signaling. Molecular Endocrinology. 2003;17: 1240–1254. doi:10.1210/ME.2002-0190

45. T Y, H S, M A-K, N Y, AH H, T M, et al. Identification of liver X receptor-retinoid X receptor as an activator of the sterol regulatory element-binding protein 1c gene promoter. Molecular and cellular biology. 2001;21: 2991–3000. doi:10.1128/MCB.21.9.2991-3000.2001

46. M B, TÅ P, B G, SJ van H, D H, C B, et al. Genome-wide profiling of liver X receptor, retinoid X receptor, and peroxisome proliferator-activated receptor α in mouse liver reveals extensive sharing of binding sites. Molecular and cellular biology. 2012;32: 852–867. doi:10.1128/MCB.06175-11

47. Kusumanchi P, Liang T, Zhang T, Ross RA, Han S, Chandler K, et al. Stress-Responsive Gene FK506-Binding Protein 51 Mediates Alcohol-Induced Liver Injury Through the Hippo Pathway and Chemokine (C-X-C Motif) Ligand 1 Signaling. Hepatology. 2021 [cited 6 Sep 2021]. doi:10.1002/HEP.31800

811 48. Manmadhan S, Ehmer U. Hippo Signaling in the Liver – A Long and Ever-Expanding Story.
812 Frontiers in Cell and Developmental Biology. 2019;7: 33. doi:10.3389/FCELL.2019.00033

813 49. Kyrmizi I, Hatzis P, Katrakili N, Tronche F, Gonzalez FJ, Talianidis I. Plasticity and expanding
814 complexity of the hepatic transcription factor network during liver development. Genes and
815 Development. 2006;20: 2293–2305. doi:10.1101/GAD.390906

816 50. Nishikawa T, Bell A, Brooks JM, Setoyama K, Melis M, Han B, et al. Resetting the transcription
817 factor network reverses terminal chronic hepatic failure. The Journal of Clinical Investigation.
818 2015;125: 1533. doi:10.1172/JCI73137

819 51. Farooque U, Lohano AK, Dahri Q, Arain N, Farukhuddin F, Khadke C, et al. The Pattern of
820 Dyslipidemia in Chronic Liver Disease Patients. Cureus. 2021;13.
821 doi:10.7759/CUREUS.13259

822 52. Oliva L, D'Incà R, Medici V, Sturniolo GC. Metallothioneins and liver diseases. Metallothioneins
823 in Biochemistry and Pathology. 2008; 289–316. doi:10.1142/9789812778949_0014

824 53. Huang G-W, Yang L-Y. Metallothionein expression in hepatocellular carcinoma. World Journal
825 of Gastroenterology. 2002;8: 650. doi:10.3748/WJG.V8.I4.650

826 54. Devisscher L, Campenhout S van, Lefere S, Raevens S, Tilleman L, Nieuwerburgh F van, et
827 al. Metallothioneins alter macrophage phenotype and represent novel therapeutic targets for
828 acetaminophen-induced liver injury. Journal of Leukocyte Biology. 2021; 1–11.
829 doi:10.1002/JLB.3A0820-527R

830 55. Lefebvre V. The SoxD transcription factors – Sox5, Sox6, and Sox13 – are key cell fate
831 modulators. The International Journal of Biochemistry & Cell Biology. 2010;42: 429–432.
832 doi:10.1016/J.BIOCEL.2009.07.016

833 56. Wang Y, Ristevski S, Harley VR. SOX13 Exhibits a Distinct Spatial and Temporal Expression
834 Pattern During Chondrogenesis, Neurogenesis, and Limb Development:
835 http://dx.doi.org/101369/jhc6A69232006. 2006;54: 1327–1333.
836 doi:10.1369/JHC.6A6923.2006

837 57. Liu L, Yannam GR, Nishikawa T, Yamamoto T, Basma H, Ito R, et al. The microenvironment
838 in hepatocyte regeneration and function in rats with advanced cirrhosis. Hepatology. 2012;55:
839 1529–1539. doi:10.1002/HEP.24815

840 58. Guzman-Lepe J, Cervantes-Alvarez E, l'Hortet AC de, Wang Y, Mars WM, Oda Y, et al. Liver-
841 enriched transcription factor expression relates to chronic hepatic failure in humans.
842 Hepatology Communications. 2018;2: 582–594. doi:10.1002/HEP4.1172

843 59. Yamagishi S, Matsui T. Role of receptor for advanced glycation end products (RAGE) in liver
844 disease. European Journal of Medical Research. 2015;20. doi:10.1186/S40001-015-0090-Z

845 60. Zeng M, Liu W, Hu Y, Fu N. Sumoylation in liver disease. Clinica Chimica Acta. 2020;510: 347–
846 353. doi:10.1016/J.CCA.2020.07.044

847 61. Garcia-Alonso L, Holland CH, Ibrahim MM, Turei D, Saez-Rodriguez J. Benchmark and
848 integration of resources for the estimation of human transcription factor activities. Genome
849 Research. 2019;29: 1363–1375. doi:10.1101/gr.240663.118

850 62. Gautier L, Cope L, Bolstad BM, Irizarry RA. Affy - Analysis of Affymetrix GeneChip data at the
851 probe level. Bioinformatics. 2004;20: 307–315. doi:10.1093/bioinformatics/btg405

852 63. Kauffmann A, Gentleman R, Huber W. arrayQualityMetrics - A bioconductor package for quality
853 assessment of microarray data. Bioinformatics. 2009;25: 415–416.
854 doi:10.1093/bioinformatics/btn647

855 64. Edgar R, Domrachev M, Lash AE. Gene Expression Omnibus: NCBI gene expression and
856 hybridization array data repository. Nucleic Acids Research. 2002;30: 207–210.
857 doi:10.1093/nar/30.1.207

858 65. Hänzelmann S, Castelo R, Guinney J. GSVA: gene set variation analysis for microarray and
859 RNA-Seq data. BMC Bioinformatics. 2013.

860 66. Fabregat A, Jupe S, Matthews L, Sidiropoulos K, Gillespie M, Garapati P, et al. The Reactome
861 Pathway Knowledgebase. Nucleic Acids Research. 2018;46: D649–D655.
862 doi:10.1093/nar/gkx1132

863 67. Liberzon A, Subramanian A, Pinchback R, Thorvaldsdóttir H, Tamayo P, Mesirov JP. Molecular
864 signatures database (MSigDB) 3.0. Bioinformatics. 2011;27: 1739–1740.
865 doi:10.1093/bioinformatics/btr260

866 68. Dolgalev I. msigdbr: MSigDB Gene Sets for Multiple Organisms in a Tidy Data Format. 2020.

867 69. Garcia-Alonso L, Ibrahim MM, Turei D, Saez-Rodriguez J. Benchmark and integration of
868 resources for the estimation of human transcription factor activities. bioRxiv. 2018; 337915.
869 doi:10.1101/337915

870 70. Smedley D, Haider S, Durinck S, Pandini L, Provero P, Allen J, et al. The BioMart community
871 portal: an innovative alternative to large, centralized data repositories. Nucleic Acids Research.
872 2015;43: W589–W598. doi:10.1093/nar/gkv350

873 71. Ritchie ME, Phipson B, Wu D, Hu Y, Law CW, Shi W, et al. Limma powers differential
874 expression analyses for RNA-sequencing and microarray studies. Nucleic Acids Research.
875 2015;43: e47. doi:10.1093/nar/gkv007

876 72. Türei D, Korcsmáros T, Saez-Rodriguez J. OmniPath: Guidelines and gateway for literature-
877 curated signaling pathway resources. Nature Methods. 2016;13: 966–967.
878 doi:10.1038/nmeth.4077

879 73. Türei D, Valdeolivas A, Gul L, Palacio-Escat N, Klein M, Ivanova O, et al. Integrated intra- and
880 intercellular signaling knowledge for multicellular omics analysis. Molecular Systems Biology.
881 2021;17: e9923. doi:10.15252/msb.20209923

882 74. Makowski D, Ben-Shachar MS, Patil I, Lüdecke D. Methods and Algorithms for Correlation
883 Analysis in R. Journal of Open Source Software. 2020;5: 2306. doi:10.21105/JOSS.02306

884 75. Dewey M. metap: meta-analysis of significance values. 2020.

885